Journal of Natural Gas Science and Engineering 82 (2020) 103521

Contents lists available at ScienceDirect

Journal of Natural Gas Science and Engineering

journal homepage: http://www.elsevier.com/locate/jngse

The early Paleozoic structures and its influence on the Permian strata, Midland Basin: Insights from multi-attribute seismic analysis

Sumit Verma *, Matt Scipione

Department of Geosciences, UT Permian Basin, Odessa, TX, USA

ARTICLE INFO

Keywords:
Seismic attribute
3D seismic
Paleozoic structures
Permian basin

ABSTRACT

The Permian Basin is one of the most important petroleum-producing regions in the United States. The structural history of the Permian Basin is extremely complex. Most of the structural traps in the Permian Basin are associated with the strike-slip fault system, which presented challenges for past structural interpretation completed primarily using well log and 2D seismic data. We utilized a 3D seismic survey, a part of the Midland Basin and eastern margin of the Central Basin Platform (CBP), to identify the Early Paleozoic structural elements to study its influence on the HC production from the Permian strata. We computed volumetric seismic attributes including, coherence which can identify faults with a significant amount of throw, along with curvature which can detect flexure and folds. We also used, recently developed aberrancy attribute, which illuminates subtle faults and flexures. We observed several strong lineations on seismic attributes extracted along the Woodford surface. Lineations have three different trends. Trend 1 lineations are drag folds associated with the Andrews shear zone (ASZ). Trend 2 lineations, which show a left-lateral strike-slip motion, are R' Riedel Shear, are oriented N 65° W truncating against the CBP. The trend 2 lineations continue upward to the shallower surfaces, as well as they are parallel to the surface lineations identified on the satellite images, which indicates the continued movement of the pre-existing faults. The trend 3 lineations, which show a right-lateral strike-slip motion, are R Riedel Shear and align with the ASZ. The formation micro image (FMI) shows the fracture orientations in trend 2 and trend 3 directions. The aberrancy lineation anomalies are indicative of highly fractured areas; wells drilled in these areas display lower oil-water ratio, as well as a higher amount of production, which may be due to the increase in permeability due to the fractures.

1. Introduction

The Permian Basin, also known as West Texas Basin, covers an extensive area in southeast New Mexico and west Texas (Fig. 1; Ruppel, 2019). The Permian Basin contains many vertically stacked oil and gas producing intervals. The Permian Basin is one of the highest (by volume) oil and gas producing regions in the United States, with cumulative production of 33 billion barrels of oil and 118 trillion cubic feet of gas (EIA, 2018). The Permian Basin consists of two main sub-basins, Midland Basin in the east and Delaware Basin in the west, separated by an NW trending uplifted basement block, known as, the Central Basin Platform (CBP). Delaware Basin and Midland Basin and the CBP have evolved from previously existing Tobosa Basin. The Tobosa Basin was a shallow Paleozoic age basin, which was present until Early Pennsylvanian. Until this time, the CBP was a low relief feature. The Ouachita orogeny began in the Early Pennsylvanian. At the end of this orogeny, the CBP became the crystalline-basement-involved (NW-SE trending) major structural high at the center of the Permian Basin. After the Ouachita orogeny, the west Texas area has not experienced any major tectonism except Cretaceous to Early Eocene aged Laramide orogeny and middle to late Cenozoic aged Basin-and-Range rift (Ewing, 2019; Hoak et al., 1998, Fig. 2). Both of these later events have no documented significant impact on CBP and the Midland Basin structure.

In the Permian Basin, most of the oil and gas are produced from the Permian aged formations. The pre-Permian aged tectonics provided the structural framework for the deposition of the Permian formations and played a significant role in forming petroleum traps. Although some of the petroleum, in Midland Basin, occur in stratigraphic traps (erosional truncations and pitchouts), most of the oil and gas traps are associated with the restraining bends in transpressional zones of strike-slip faults, and small anticlines associated with faults (Hoak et al., 1998). Bolden (1984) studied different surface lineaments on satellite images and

* Corresponding author.
E-mail address: sumit.verma.geophysicist@gmail.com (S. Verma).

https://doi.org/10.1016/j.jngse.2020.103521
Received 8 April 2020; Received in revised form 26 July 2020; Accepted 27 July 2020
Available online 7 August 2020
1875-5100/Published by Elsevier B.V.

found a correlation with the Paleozoic tectonics. Most of the producing petroleum fields between Concho and Double Mountain lineaments are oriented in a certain direction. This orientation can be explained by a strike-slip system. Tai and Dorobek (2000) used the right-lateral strike-slip system model, proposed by Yang and Dorobek (1995), to explain structural features present at the Paleozoic level in the eastern CPB and western Midland Basin. Although tectonics has played a significant role in trapping oil and gas in Midland Basin, there has been a limited number of studies on the influence of pre-Permian tectonics on the deposition of Permian formations and origin of the structural features present in the Permian Basin (Ruppel, 2019). In this paper, we attempt to improve our understanding of pre-Permian tectonics and its influence on the Permian strata. We also, attempt to study the impact of the pre-Permian tectonics on the production of oil and gas in our study area (Fig. 1a). Our study area lies on the eastern margin of the northern CBP and extends Midland Basin to the East.

Most of the geologists use the strike-slip (wrench) model to explain the faults and folds present in the Permian Basin. In general, very long

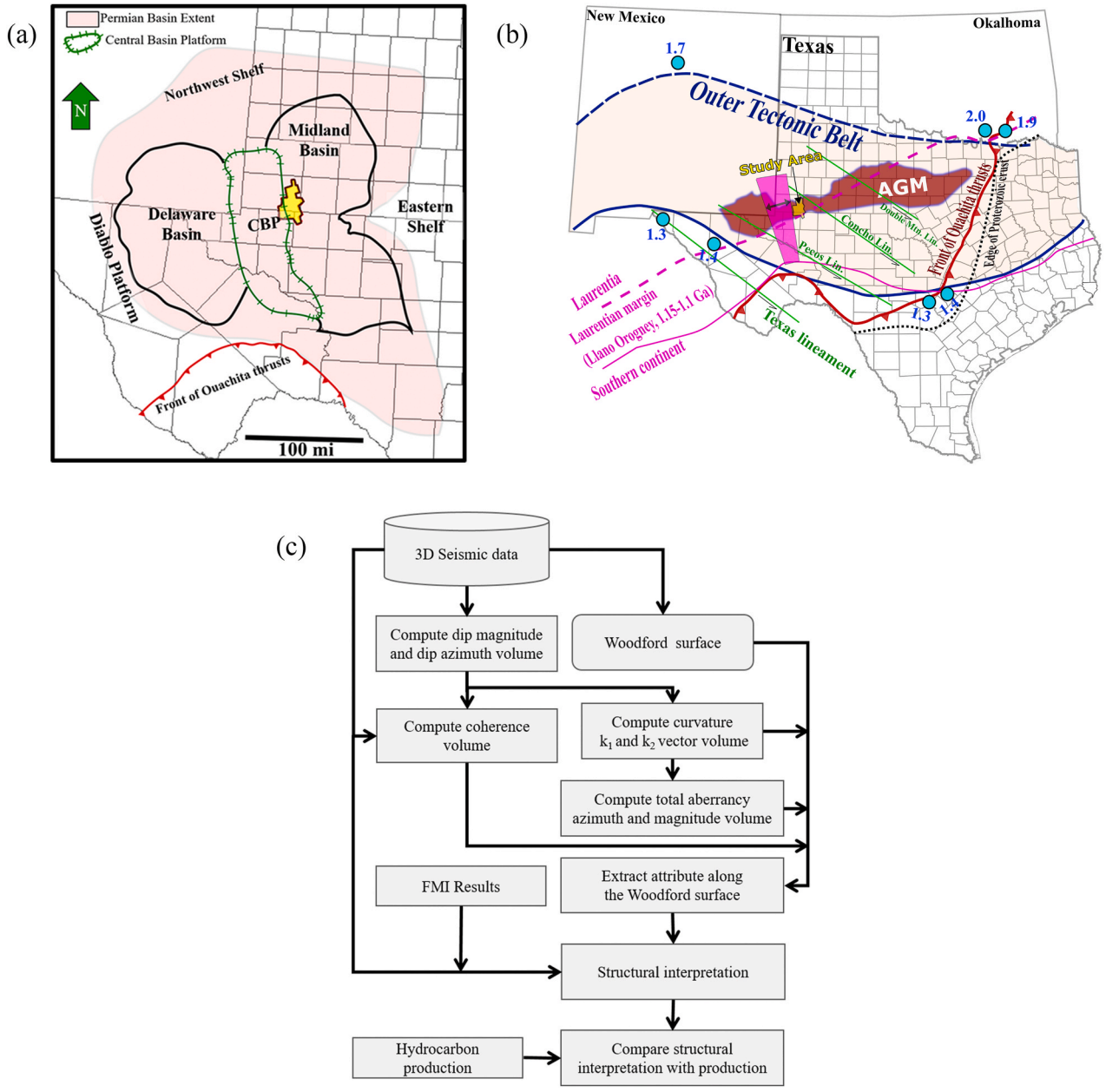

Fig. 1. (a) Map view of the study area along with the outlines of Permian Basin, Delaware Basin, Midland Basin, Central Basin Platform (CBP). The study area is displayed with a polygon filled with yellow (modified from EIA, 2018). (b) Figure displays different structural features, which have evolved from Precambrian to Early Permian. The formation of the outer tectonic belt occurred (the area shaded with light orange), which between 1.7 and 1.6 Ga. At the rim of the Outer Tectonic Belt, the cyan circles are posted with a number posted next to it. The number represents the age in Ga of the oldest rocks found at the location. The edge of the Proterozoic crust is marked as a dashed black line. The Abilene gravity minimum (AGM) is represented by a red colored solid filled polygon. The magenta lines (dashed and solid) represents the tectonic reconstruction of the Texas Precambrian collision from 1.15 to about 1.07 Ga causing extension as well as uplift. The magenta polygon represents the extension, which was filled by Pecos complex. Texas lineaments are NW-SE oriented solid lines. The black solid lined polygon is the outline of the Central Basin Platform (CBP). The yellow polygon represents the location of the study area, falls in the transition zone of the outer tectonic belt. Also, notice that most of the survey area is on the AGM, however in the southeast, the seismic survey covers little more area after the edge of the AGM. (modified after Adams and Keller, 1996; Ewing, 2016; Ruppel, 2019; Bolden, 1984). (c) Workflow for the structural interpretation used in this study.

lineaments, steeply dipping faults, en échelon nature of faulting characterize the strike-slip fault system (Bolden, 1984). Fault trends, strike-slip movement, and other lateral relations can only be inferred from well control and 2D seismic data. Stratigraphic horizons traced using 3D seismic surveys can discern such structures with greater certainty. During the past 30 years, 3D seismic surveys have given geologists a new tool to analyze relationships of faults and other tectonic features in areas in which such features cannot be observed in outcrop. In the past 20 years, several seismic attributes have been developed, which are computed on 3D seismic surveys. Geoscientists have utilized such seismic attributes effectively to illuminate the structural and stratigraphic features which were difficult to infer from conventional

(a)

Era/ Period	Formation CPB/MB	Orogeny/Rift Age (Ma)	Tectonic Phase
Quaternary	Holocene sand	25-5	Quaternary faulting
Neogene			
Paleogene		70-30	Laramide Orogeny
Mesozoic			
Permian			
	Wolfcamp	325-275	Ouachita Orogeny
Pennsylvanian	Cisco		
	Canyon		
	Strawn		
	Atoka		
Mississippian	Barnett		
	Miss. Lime		
Devonian	Woodford		
Silurian			
Ordovician			
	Ellenburger		
Cambrian	Cambrian	~550	Eocambrian Rift
Neo Proterozoic			
		1300-1100	Grenville Orogeny
Meso Proterozoic		1330-1260	Pregrenville Extension
		1700-1400	Outer Tectonic belt

(b)

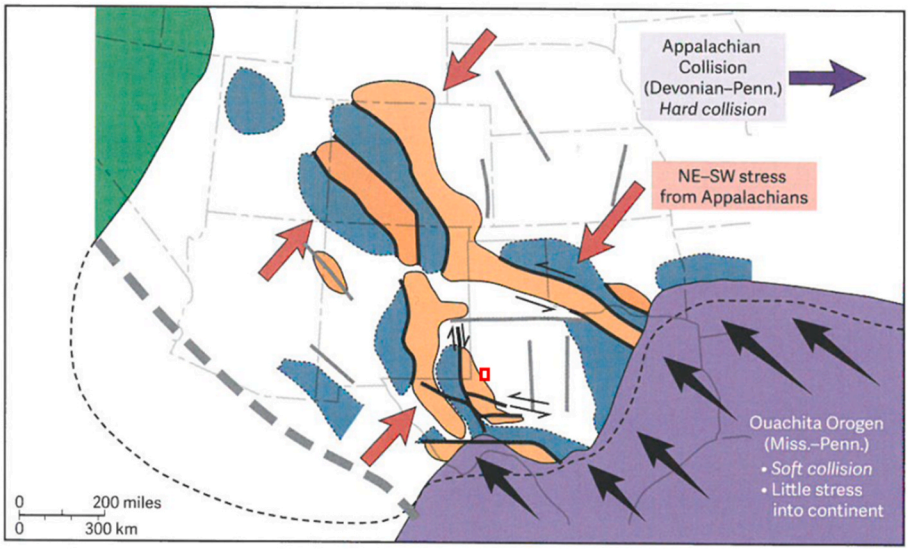

Fig. 2. (a) Stratigraphic chart, displaying different tectonic events their ages. In the section column CBP= Central Basin Platform, and MB = Midland Basin. Second column shows the formations which were deposited during different tectonic phases. In the second and third columns, the red color = orogeny, and blue color = rifts. (b) Displays the convergent vectors as well as major shorting that took place in the southern North America during the Ouachita orogeny (modified after Ewing, 2016).

amplitude volumes (Chopra and Marfurt, 2007; Bhattacharya and Verma, 2020). Pu et al. (2019) utilized seismic amplitude along with seismic attributes to interpret to characterize the strike-slip fault system in Tarim Basin, China. Although, the high quality 3D seismic surveys have allowed the Permian Basin geologists to study and understand the structural complexities, however, such studies are mostly unpublished due to the proprietary nature of the work (Adams and Keller, 1996; Ewing, 2019). There are very few publications, which utilize seismic attributes to support the structural interpretation in Permian Basin (Blumentritt et al., 2003; Bhatnagar et al., 2019). In this paper, we utilize the modern seismic attributes, including curvature and aberrancy to understand the structural features including their origin and their impact on hydrocarbon production.

Our study aims to characterize Lower Paleozoic structures associated with the Ouachita orogeny and the uplift of CBP. In this paper, first, we describe the structural evolution of the Permian Basin from the Precambrian through the Paleozoic. Second, in the methodology section, we provide an overview of the 3D seismic data, and workflow of computing seismic attributes including coherence, curvature, and aberrancy along a known surface (Fig. 1c). Third, in our results section, we use the seismic attributes to highlight faults and different lineaments. The use of seismic attributes provides a significantly better definition of structural features. In addition, we display structural features seen on the well-based Woodford surface depth surface along with the production wells. Fourth, we attempt to correlate the faults and lineaments identified with seismic attributes and petroleum production in a discussion section. Finally, we conclude with the results of the study area and overall structural interpretation of the features seen within the 3D Seismic.

2. Structural history

West Texas has experienced different tectonic events starting from the outer tectonic belt orogenic event (1.7–1.4 Ga). Fig. 2a lists all the major orogenic and rifting events in this region. The following geological features are important for our study: the Precambrian basement, Abilene gravity minimum (AGM), the Texas lineaments, Grenville front, and Ouachita orogeny (Fig. 2a); we will discuss these features in this section.

2.1. Precambrian basement

In most of the continental areas of North America, the Precambrian basement acts as a structural basis. In general, the petroleum exploration targets are the younger Phanerozoic basin, and such younger rock structures conceal the Precambrian basement. In the Permian Basin, Precambrian basement faults are present, which are the result of Precambrian tectonics. Ouachita orogeny rejuvenated these basement faults in Pennsylvanian, which controlled the Permian sedimentation and structures, and plays a significant role in the distribution of source and reservoir rocks (Adams and Keller, 1996). Although most of the sediments in the Permian Basin deposited in the Paleozoic era, the controlling structural elements are Precambrian in age. In order to understand the present-day structure of the Permian Basin, one must evaluate the tectonostratigraphic framework from the Proterozoic and Paleozoic (Fig. 2a; Hoak et al., 1998).

2.2. Abilene gravity minimum

The Abilene gravity minimum (AGM) trends east-northeast and is 400 km long gravity anomaly feature (Fig. 1b). The AGM appears due to a granitic batholith in the subsurface and extends from Dallas, Texas area in the east to the Delaware Basin in the west (Adams et al., 1993; Ruppel, 2019). In this area, the less dense granite batholith intrudes the dense Precambrian metamorphic rocks, resulting in a low gravity anomaly. Adams and Keller (1996) proposed that the AGM causing batholith is a continental margin arc batholith (north of the Llano uplift) of Middle Proterozoic age. The AGM marks the boundary between the predominantly granite-rhyolite basement in the north to metamorphic rocks in the south (Mosher, 1998). The AGM trends directly through the study area creating a potential conduit for heat flow, increasing maturation during the Phanerozoic.

2.3. Texas lineament

Many NW-SE trending surface lineaments observed on satellite image e.g. Concho lineament, Pecos lineament, the Texas lineament, and others (represented by green solid lines in Fig. 1b; Bolden, 1984). Among, the lineaments the Texas lineament is more studied. It is approximately oriented around $N54^{O}W$ and displays a left-lateral strike-slip motion (Swan, 1976). The approximate age of the initial movement of the Texas Lineament is 1.4 Ga. Continued movement on these N 60° W trending faults can be seen through the Laramide and today (Muehlberger, 1980).

2.4. Grenville front

The east-west trending Grenville orogeny contains both arc-continent and continent-continent collision tectonic activities (Figs. 1b and 2a). In Texas, Llano uplift is one of the more studied events caused by Grenville orogeny. Grenville-age rocks are essential in completing plate reconstructions for Neoproterozoic supercontinent Rodinia. Most of the plate reconstructions of Rodinia miss to include a southern continent off of the southern boundary of Laurentia. In Fig. 1b, the solid magenta line represents the northern edge of this southern continent. The southern continent collides with Laurentia around 1.15–1.12 Ga causing the Llano uplift in Texas. The collision created a rift perpendicular to this collisional margin at a block, which would later be uplifted to create the CBP (Mosher, 1998). Post Grenville through the Lower Paleozoic, the Permian Basin region (which was Tobosa Basin at that time), set up in a passive margin succession, which had a gently dipping slope.

2.5. Ouachita orogeny (Central Basin Platform uplift)

The Ouachita orogeny, also known as Marathon Ouachita orogeny, is a collision of North America and Gondwana land (Africa and South America). The contact initiated on eastern margin North America then through Texas (Fig. 2b). The Ouachita orogeny had three-phase of tectonics, the first one occurred in late Mississippian (depositional time of Barnett Shale), the second one in early Pennsylvanian (depositional time of Atoka Formation) and the third on in mid-Pennsylvanian (Strawn Formation). The first phase of uplift began in late Mississippian with the Precambrian NW trending fault system reactivation (Hoak et al., 1998). In the second phase, during the Early Pennsylvanian, the contraction touched its peak, forming through basement wrench faults. Ballard (2014) analyzed the structural highs in the Permian Basin area (Fig. 3a). He concluded that some of the structural highs suggest major basement involved folding in Early Pennsylvanian.

2.6. Andrews shear zone

Gardiner (1990) observed a NE trending zone of low gravity (and low magnetic) anomaly, between two gravity (and magnetic) highs, and named it Andrews Shear Zone or ASZ (Fig. 3a). The ASZ represents a primary structural margin of the basement. The ASZ area is dominated by the faults and folds oriented in NE direction and displays right-lateral strike-slip movements. The en échelon folds associated with ASZ (with NE orientation) were documented in Andrews and Crosby county Texas, provides additional support. The ASZ is around 15–20 km in wide and extends in an area of ~850 mi^2 (Hoak et al., 1998).

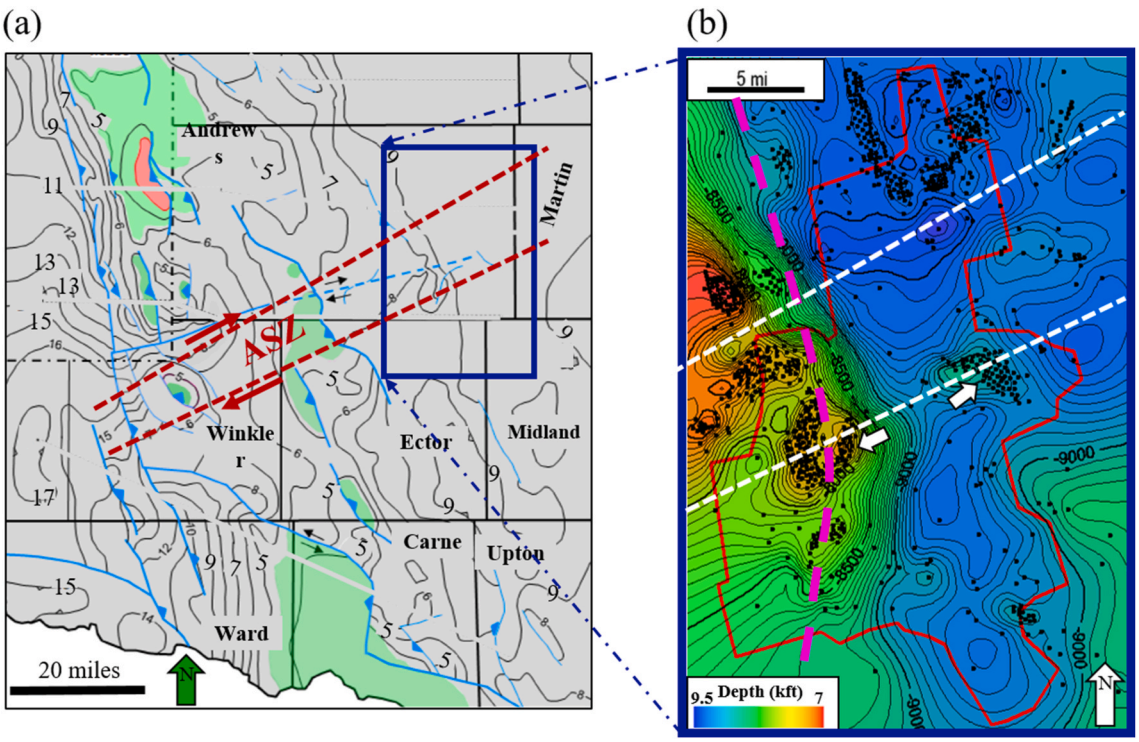

Fig. 3. (a)Structure map of the top of the Devonian 31 Formation on the Northern Central Basin Platform with the study area outlined in blue. The light blue lines delineate major faults on the platform (modified from Ballard, 2014). The dotted red lines shows the Andrews Shear Zone (Hoak et al., 1998; Gardiner, 1990) (b) A structure map of the top of Woodford generated using well logs. The black dots indicate the location of the wells used. The contour intervals represent 100 feet in subsea values. The warmer colors (red-orange) indicate the shallower depths while the colder colors (green-blue) indicate deeper depths of the Woodford formation. The dashed magenta line on the map represents the approximate location of the CPB's eastern margin.

2.7. Structural history of the study area

Most of the studies done on the structural history of the CBP have been in the southern margin, but similar structural styles are co-relatable to the north. During the Pennsylvanian phase of Ouachita orogeny, right-lateral shearing in zones of transpression created en échelon faulted anticlines on the southern margin and western margin of the CBP. The suture, between CBP and South America, was not proximal to the CPB in the early Pennsylvanian (Ballard, 2014). We do not completely know how the convergent vectors and Ouachita front uplifted the CBP. Convergence from the southwest can explain the transpression on the western margin of the platform. In the late Pennsylvanian-Wolfcampian period, which is the last phase of Ouachita orogeny, strain partitioning continued and right-lateral oblique-slip occurred on the western margin of the CBP. This phase of the orogeny reactivated the basement faults. Also during this time-period majority of the uplift of the CBP occurred (Tai and Dorobek, 2000). The reactivated Proterozoic basement faults create a rotational bulk strain in the sediments above and drive strike-slip tectonics. This rotational strain on the overburden can create different structures in the lower Paleozoic formation such as thrust faults, normal faults, folds, and Riedel shears. All these structural elements are present on the CBP.

Ballard (2014), noticed the basement derived thrust faults are the most common features on the northern CPB, which trend NNW. Ballard (2014) also observed strike-slip faults, which have two primary orientations, which are NW or NE (Fig. 3a). The NW trending faults display a left-lateral displacement, whereas NE trending faults display a right-lateral displacement. Andrews Shear zone has the right-lateral displacement. It is not clear how NW-SE compression indirectly affected uplift. Different authors have tried to explain it with either strike-slip motion, block rotations or the reactivation of basement faults. The western Midland Basin and eastern margin of the CBP contain numerous NW-SE trending en échelon folds and faults, Tai and Dorobek (2000) proposed that these structures formed under the right-lateral strike-slip deformation with an additional component of compression, during the last phase of Ouachita orogeny.

3. Data and methodology

3.1. Seismic survey and well logs

Our study area, which includes parts of Andrews, Ector, Midland and, Martin County covering a total area of 440 mi^2. The study area is covered by a mega-merge 3D seismic survey (Figs. 1a and 4). The mega merge seismic survey consists of fourteen different seismic surveys. These smaller surveys were acquired in a span of twenty years (the oldest being 1996), using instruments and technologies present at that time. All of the seismic surveys were merged and reprocessed to generate pre-stack time migrated volume, with the 2 ms sample rate at the bin size of 110 feet × 110 feet (Bhatnagar et al., 2019). Further, these processed seismic data were stacked. We only had access to the mega-merge stacked seismic dataset. The overall seismic data quality is moderate to poor compared to the current seismic technology. There are several reasons for such data quality. The older surveys were acquired with irregular and coarse grids, with a narrow range of source frequencies. The original seismic surveys have different offset ranges and nominal folds, such difference leads to different data quality in different parts of the merged seismic survey (Verma et al., 2013). We also have access to over 400 wells, which penetrate the Woodford formation. We utilized the well tops to create a Woodford depth surface (Fig. 3).

3.2. Seismic survey and fault identification

One of the first objectives when interpreting new seismic data is to identify the major faults. In general, faults with large throws are imaged well in 3D seismic surveys but small throw (or sub-seismic) faults are

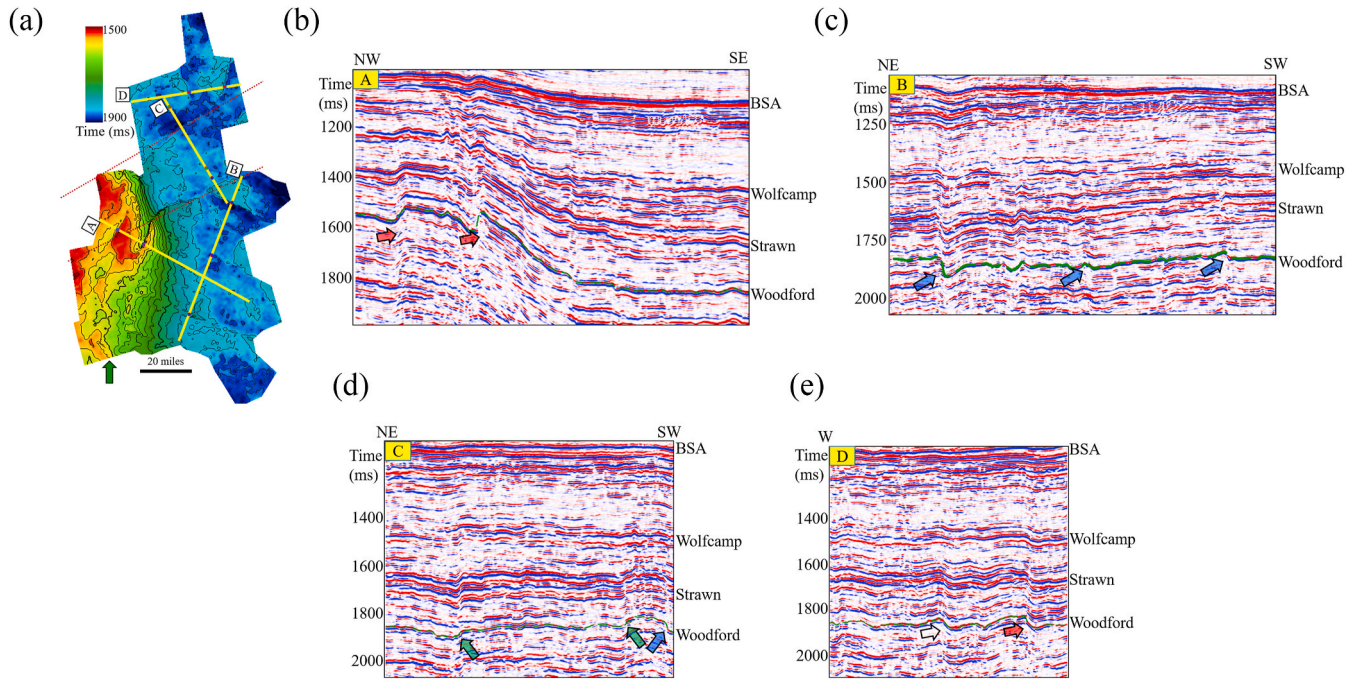

Fig. 4. (a) The Woodford formation time structure map, the warmer colors (red-orange) indicating the shallower depths while the colder colors (green-blue) indicate deeper depths. The dotted red lines show the extent of Andrews shear zone (ASZ). The solid yellow lines, represent the vertical cross sections A (in Fig. 4b), B (in Fig. 4c), C (Fig. 4d), and D (in Fig. 4e). The solid dots on the yellow lines match the location of the arrows of the same color on the corresponding vertical cross section. (b) A vertical cross-section oriented NW-SE, from the eastern edge of CBP to Midland Basin. The red arrows display the location of the bend or fault, oriented NE-SW. Note that the bend in the strata continues shallower horizons. Note BSA is base of San Andres horizon. (c) A vertical cross section oriented NE-SW in the Midland Basin. The blue arrows display the location of bends in strata oriented NW-SE. (d) a vertical cross section oriented NE-SW in the Midland Basin. The green arrows display the location of the faults, oriented NE-SW. (e) a vertical cross section oriented W-E, in the northern part of the survey.

less well imaged, while joints are typically not imaged at all. Petroleum geologists are interested in sub-seismic faults and areas of fractures as they can dramatically increase the permeability in both conventional and unconventional reservoirs. Geometric attributes such as reflector dip, curvature, and aberrancy combined with coherence can help us identify sub-seismic faults and possible fractures zones (Bhattacharya and Verma, 2019; Chopra and Marfurt, 2007).

3.3. Dip magnitude and azimuth

Precise estimations of reflector dip magnitude and dip azimuth are necessary for correct estimation of geometric attributes such as coherence, curvature, and aberrancy (Fig. 5). The dip attribute represents the dip direction (dip azimuth) and plunge (dip magnitude) of a bed (reflector). In our implementation, we compute the reflector dip by a robust dip search method described by Marfurt (2006). Such volumetric dip is useful in the delineation of folds, faults, fractures, karsts, channels, and differential compactions (Blumentritt et al., 2003).

3.4. Coherence

Coherence attributes compare seismic waveforms and/or amplitude in adjacent traces. There are different types of coherence estimates of similarity based on different algorithms, the list may include cross-correlation, semblance, variance, Eigen structure, and Sobel filter (Chopra and Marfurt, 2007). For our study, we compute Sobel filter similarity along the dip of seismic reflectors (Bhatnagar et al., 2019). Sobel filter similarity is used in image processing packages as an edge detection filter, which scans the data horizontally and vertically to map discontinuities. In subsurface imaging with seismic, Sobel filter similarity is used to map discontinuous features such as channels edges, faults, and fractures. Sobel filter detects the break in reflector configuration or lateral changes in amplitude values and waveform shape and provides enhanced image of faults and lineaments (Li et al., 2017; Bhattacharya and Verma, 2020). Such discontinuities are associated with abnormally low values of coherence and are called coherence anomalies. Coherence, cannot detect a fault, which does not have a break in reflector (Fig. 5). It is one of the limitations of coherence. In such situations, we can study other seismic attributes.

3.5. Structural curvature

Structural curvature measures how curved (bending and folding) a certain structure is, based on the structures dip. Mathematically, it is the second derivative of structure or a derivative of dip. The structural curvature attribute is most commonly used for understanding structural complexity (faults and fractures) and highlighting the footwall and hanging wall of distinct faults (Marfurt and Alves, 2015). In a 2D cross-section, an antiform (peak) will display a positive curvature anomaly, whereas a synform (trough) would display a negative curvature. A bed with a constant dip (slope), or where the structure is not bending, will display a zero curvature. Two principal curvatures are required to represent a 3D structure. Such curvatures can be, most positive principal, k_1 and most negative principal, k_2 curvature accounting for structural complexity in 3-dimensional domain. It should be noted that the k_1 and k_2 values calculated are principal curvatures. That means, for an asymmetric or recumbent fold the k_1 anomalies would appear along the hinge line of a fold as opposed to the limb (which are denoted by k_{pos}). Therefore, the k_1 and k_2 curvature values presented in this work represent the geologic features highlighting the peak of an anticline and the trough of a syncline. In our computation of curvature, apart from the magnitude of the curvature, we find the strike of curvature. For a fold, the strike of a k_1 would be the direction of the fold axis (Chopra and Marfurt, 2007; Mai, 2010; Verma et al., 2018).

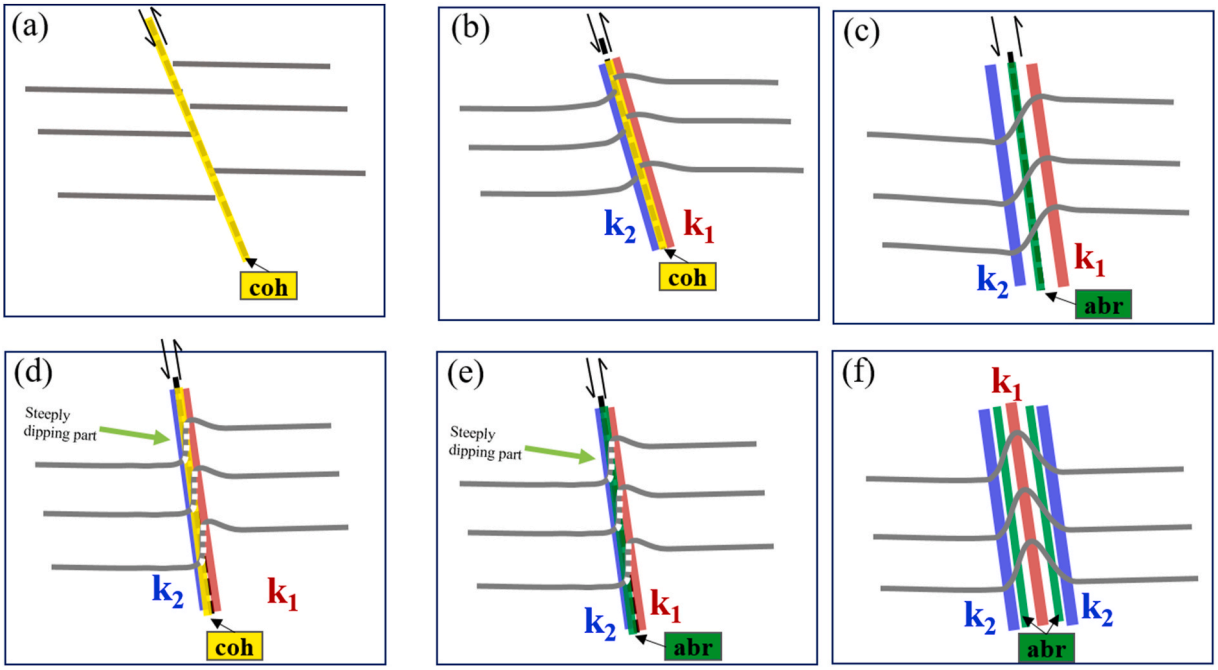

Fig. 5. Seismic attributes (coherence, curvature and aberrancy) response to different reverse faults and folds. (a) Coherence (coh) illuminates a reverse fault with significant throw offset; here there is no folding of strata is present, hence there are no curvature or aberrancy anomalies. (b) Negative-curvature (k_2) anomaly illuminated on downthrown block and positive-curvature (k_1) anomaly illuminated on the upthrow block, for a reverse fault with significant folding. Coherence anomaly occurs at the fault; curvature anomalies (k_1 and k_2) brackets the coherence anomaly. (c) Monoclinal fold in strata, with no visible break in reflector, so no coherence anomaly. However, k_1 anomaly occurs on the up thrown block and k_2 anomaly on the downthrown block; the aberrancy anomaly occurs at the center of the ramp. (d) Steeply dipping reverse fault: the steeply dipping portion is poorly images by seismic, and the waveform shape as well as the amplitude changes at the location of the fault, and coherence anomaly appears at the location of the fault. k_1, and k_2 anomalies are present on the upthrown and downthrown blocks respectively. (e) The same model as Fig. 5d, the aberrancy anomaly also occurs, at the location of the coherence anomaly. (f) Horizontal inclined fold: k_1 anomaly occurs at the hinge line (peak), whereas the aberrancy anomalies are present on both of the fold limbs, similarly k_2 anomalies occur at the hinge line (trough) (after Qi and Marfurt, 2018; Verma and Bhattacharya, 2019).

3.6. Aberrancy

The aberrancy is a relatively new seismic attribute, in terms of its applications on geoscience problems as well as publications. The dip is the first derivative of structure and the principal curvatures are second derivatives of structure, whereas aberrancy, often called flexure, is the third derivative of structure (Qi and Marfurt, 2018; Bhattacharya and Verma, 2019). The solution of such a third-order differential equation leads to three roots. Qi and Marfurt (2018) combined the three roots to define that total aberrancy vector, which can be measured by total magnitude and total azimuth. The total magnitude expresses the intensity of surface deformation, whereas the total azimuth shows the direction in which the curvature decreases in signed value. Verma and Bhattacharya (2019) describe aberrancy as not only detecting major faults that exhibit finite displacement but also can image subtle "sub--seismic resolution" faults that might be considered flexures (Fig. 5). Verma and Bhattacharya (2019) used the total aberrancy vector for structural interpretation. Lineaments in the total aberrancy vector horizon slices are indicative of potential faults or flexures (Qi and Marfurt, 2018).

3.7. Attribute extraction along the surface

In general, structural geologists recommend to perform the structural interpretation, especially for fault identification and interpretation on time slice. When we analyze the faults, which have significant throw (with seismic amplitudes or instantaneous attributes), such recommendation has a high value. However, in case of a below seismic resolution fault, one would benefit more by analyzing the data along a surface. The seismic data contains noise, but at the reflectors, the signal strength is stronger, which results in high signal to noise ratio at the reflectors. The Woodford top is a strong reflector, as well as the Woodford strata has experienced both the Early Paleozoic and Late Paleozoic tectonic deformations (Fig. 4a). We extract, all the attributes, along the Woodford top surface. These attribute extracted surface slices are also called attribute horizon slices.

3.8. Multi-attribute display

Commonly, geoscientists plot a single seismic attribute along the surface for the interpretation of geological features. For example, we can plot the dip magnitude attribute along the Woodford top surface. Such plots can be on a monochromatic or a non-cyclic multicolor scale, to show the lateral variations of dip. Similarly, dip azimuth can be plotted with a cyclic color bar, to represent the dip direction. However, we can avoid the need for two different plots, by plotting the dip and azimuth together. One of the more effective ways of doing so, is by putting the dip azimuth on the cyclic rainbow color bar and putting the dip magnitude on a black (or gray) color scale. We apply linearly varying opacity on the dip magnitude, such that the highest value of dip is transparent, and the lowest values of dip are completely opaque. In this way, the dip azimuth-dip magnitude map will display bright colors of the dip directions for the highly dipping beds, whereas the area of low dips will be dark (black or gray).

4. Results

4.1. Woodford depth surface

The Woodford Shale deposited in the Late Devonian in the Tobosa

Basin, just prior to the Ouachita orogeny. We created a Woodford depth surface using the wells (Fig. 3b). The Woodford surface shows shallowing of the contours in the southwest. The high density of contours in the west shows the steep dips, which demarcates the CBP and Midland Basin. We also, observe few small anomalous highs in the Midland Basin and CBP; the structural highs have a higher density of wells. Two of such elongated dome-shaped structural highs, indicated by white arrows in Fig. 3b, are separated by a valley; the orientation of the combined structural feature is WSW-ENE. This structural feature may have a connection to the platform and potentially influenced the elevation of the northern part of the survey area. In the south of the basin, the structural trend and orientation changes to a more ESE-WNW.

4.2. Structural lineaments on seismic attribute maps

In order to differentiate between various structural trends in the study area, we analyzed different seismic attributes along the Woodford top surface. We observed three different structural trends: trend 1, trend 2, and trend 3.

Trend 1 lineaments (thick red solid line, on Fig. 6a and b) displays strong coherence anomalies. The aberrancy, curvature and dip show and strong anomaly for trend 1 (Fig. 6c and d and 7). Trend 1 features may be the drag folds (which runs parallel to the fault, with a small offset), related to the ASZ. Not only does aberrancy illuminates the en échelon fold (similar to Verma and Bhattacharya, 2019) but also other associated lineaments correlated to the ASZ. On the aberrancy horizon slice in Figs. 6d and 7a, one can notice that the extent of the fold itself affects the structure miles further to the east compared to what was visible on the coherence. We also observed two NNE-SSW trending lineaments (marked with red dashed line); one of these lineaments is on the CBP, whereas the other one is on the northern end of the survey. We can see the corresponding vertical section of CBP lineament in Fig. 4b left red arrow, to study the nature of the lineament. It is clear that this lineament is a bend in structure and similar to the model presented in Fig. 5c. The left read arrow in Fig. 4b indicates a clear break in reflector at the level of Woodford, whereas at the level of Wolfcamp only bend in reflector is visible without any breaks. The fold at the right red arrow (in Fig. 4b), shows that, the bend becomes gentler with decreasing depth. We see a similar type of bend in structure for the lineament in the northern part of the survey (see Fig. 4e). The two lineaments only show a weak coherence anomaly but display strong aberrancy and curvature anomalies. Such features can potentially have fracture swarms and lead to areas of higher permeability or potential geohazards.

Coherence, aberrancy, and curvature horizon slices, Figs. 6 and 7, also display four distinct trend 2 lineaments-oriented WNW-ESE (thick, blue, dashed lines). On Fig. 4c the left arrow shows that, at the level of Woodford slight break is present in the reflector along with a steep bend (similar to Fig. 5d and e), at shallower horizons (e.g. at BSA) the bend has higher wavelength. Trend 2 lineaments, are Trend 2 lineaments are parallel to Bolden's (1984) and Hoak et al. (1998) wrench faults interpreted from Landsat and air photo data provided by NASA; Fig. 6b shows this lineament as magenta-colored solid lines, with number 2. Trend 2 aligns with the Concho lineament (Fig. 1b). The trend 2 lineations terminate as they approach the CBP edge. It indicates that the uplift of the CBP overprints trend 2 features and the uplift occurred after the movement on faults.

In Fig. 6 b, the Hoak et al.'s (1998) defined the Andrew shear zone (ASZ) is plotted, and ASZ completely aligns with the trend 3 lineaments. Trend 3 lineaments do not show significant coherence anomaly (Fig. 6a and b), whereas a very strong curvature and aberrancy anomaly (Fig. 6c and d, 7). Fig. 4d displays the continuity of the bends in the shallower horizons. The amplitude of the bend (fold) decreases with shallowing.

5. Discussion

5.1. Effects on shallower formations

Bhatnagar et al. (2019) discussed an MTD in an upper Leonardian formation (Fig. 8a). The primary structural feature identified using the curvature attributes is the drag fold associated with the ASZ labeled as a "curved arm." The curved arm aligns with the trend 1 drag fold in Figs. 6 and 7. The presence of the trend 1 structures in upper Leonardian aged formation, indicates the continued movement. Also, such tectonic may have supported the mechanism for driving the mass transport deposit along with the high angle dip of the structure.

The base of San Andres (BSA) is easily identifiable throughout the survey. The BSA occurs in the Guadeloupian, well after the end of the Ouachita orogeny, and is an ideal horizon to study the continued structural influence of the prior tectonics. In Fig. 8b and c, with the most positive curvature and total aberrancy, trend 1 (red) is easily identifiable. The paleotopography potentially controls the depositional environment of the San Andres formation. Trend 2 (blue) has a weak appearance on k_1 and total aberrancy. This indicates the movement along these lineaments occurred primarily during the lower Paleozoic slowed down greatly in the Guadeloupian. Trend 3 (green) can be seen to the north as an axis to the ASZ which is illuminated on both k_1 and total aberrancy. This indicates that there is a significant movement along the preexisting structures associated with trend 1, and trend 3 during the Permian time-period.

5.2. Fracture trends from FMI

The Midland Basin contains many multiple fracture trends. This is supported on a regional scale by work done by Forand et al. (2017; Fig. 9), which used FMI data throughout the Midland and Delaware Basins from various operators to create the map. In Midland Basin, they used image logs and cores on over 25 wells, in Spraberry (Leonardian in age), and Wolfcamp formation, to identify fracture height, orientation, fill, aperture, and stress orientation. They obtained fracture orientation of the open and healed fractures from the FMI logs to identify regional fracture trends (Fig. 9). Fractures trends across the Midland Basin are very similar. Most of the fracture sets are healed with calcite and have vertical to near vertical dips. In the majority of formations there tends to be a dominating fracture trend. However, in the Wolfcamp and older formations there are two orthogonal fracture sets and tend to be sporadic (Forand et al., 2017). The fracture intensity systematically varies and are in direct relation to the presence of faults (Pollock et al., 2018). On the two of the wells near study area (Fig. 9a), the orientation of the healed (and open) fractures regional is approximately N 45° E (ranging from N 30° E to N 60° E) which is close to the trend 3 (N 50° E). The secondary trend of fractures (N 50° W) on the well near survey area is very close to the trend 2 (N 65° W).

5.3. Strike-slip fault system

The right lateral strike-slip system, explains all the structural features observed in our study area as proposed by Tai and Dorobek (2000). In a strike-slip fault tectonic settings, along with the main strike-slip faults there are five different sets of fractures can form, 1) Riedel R strike-slip shear faults, 2) conjugate Riedel R' strike-slip shear fault, 3) secondary synthetic strike-slip faults P, 4) extension fractures or normal faults which develop at 45° to the principal displacement zone, and, 5) faults parallel to the principal displacement zone (Sylvester, 1988, Fig. 10).

We have found two strong lineations, the trend 2 in N 65° W and trend 3 in N 50° E. Trend 2 is similar to Ballard's (2014) NW strike-slip faults, whereas trend 3 to NE strike-slip faults. The trend 3, which is parallel to the ASZ deformation, is a right-lateral strike-slip fault (Fig. 3). The direction of trend 2 is very close to the surface lineaments orientation (N 55° W) which documented to be a left-lateral strike (Bolden,

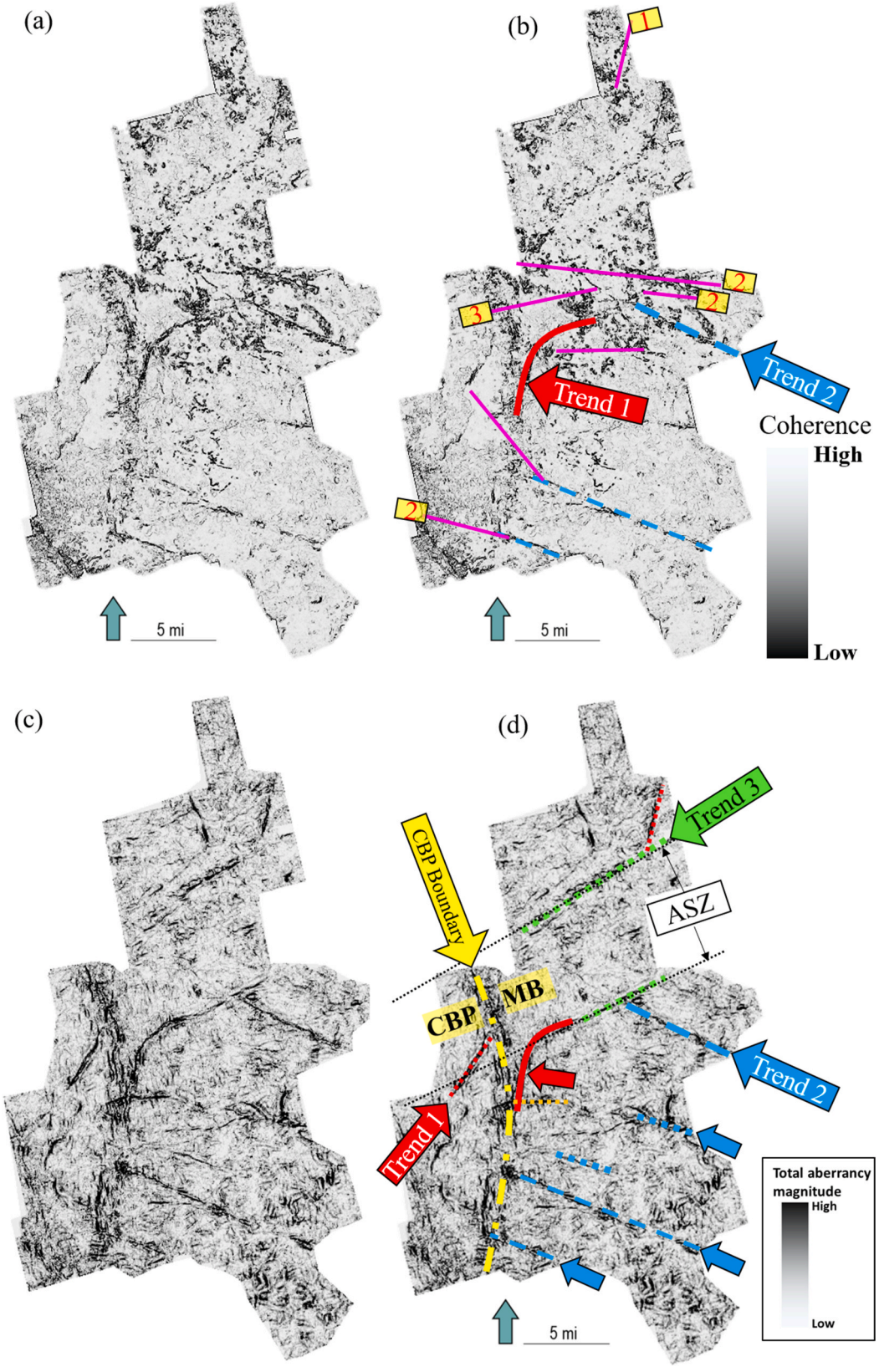

Fig. 6. Coherence calculated along the Woodford surface, (a) uninterpreted, (b) interpreted. Aberrancy calculated along the Woodford surface, (c) uninterpreted, (d) interpreted. Note, thick, solid and dashed red lines are trend 1 drag fold; thick dashed blue lines are trend 2 aligned WNW-ESE; dotted green lines are trend 3 aligned WSW-ENE. The N–S trend highlights the margin of the Central Basin Platform. The magenta colored solid lines on Fig. 6a represent the surface lineations obtained from Bolden's (1984) publication.

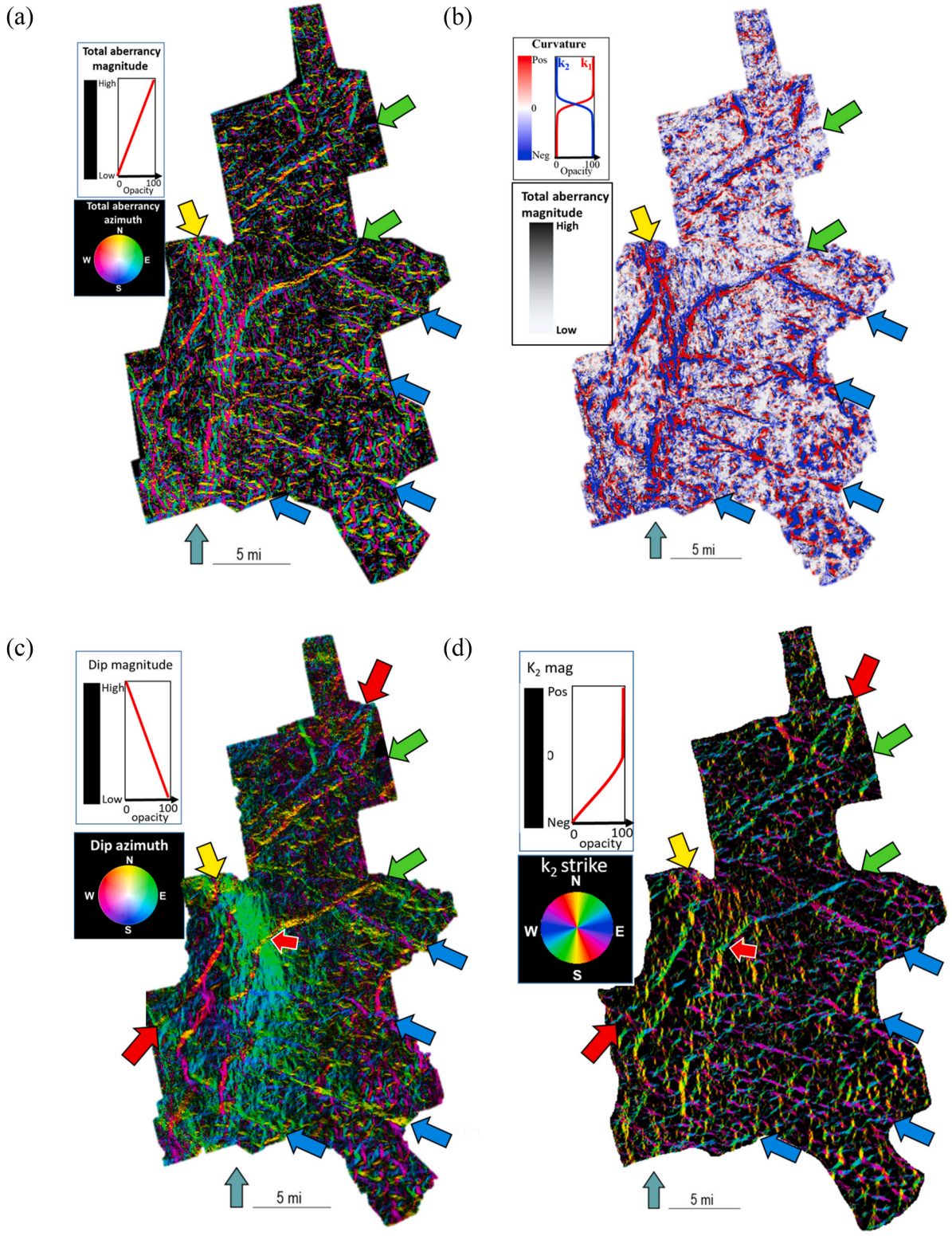

Fig. 7. Seismic attributes calculated along the Woodford surface, (a) aberrancy azimuth modulated by aberrancy magnitude; (b) aberrancy magnitude corendered k_1 and k_2 curvature, (c) dip azimuth modulated by dip magnitude, (d) k_2 strike modulated by k_2 magnitude.

1984). There may be a ~10° clockwise rotation on the fault system. The secondary trend of fractures in Permian aged formation also supports the idea of clockwise rotation.

The trend 2 and trend 3 have an angle of 60°, between them (Fig. 10a). In a right-lateral strike-slip system, the two trends perfectly fit as, trend 3 being R shear and trend 2 being R' shear. We further compare the orientation of CBP with respect to the strike-slip system; the maximum principal stress (σ_1) acts perpendicular to the orientation of the CBP. Evaluation of the direction of dip and orientation of the faults, they closely represent an intermediate stage strike-slip zone using the right-lateral strike-slip modeled by Sylvester (1988; Fig. 10). The structural highs, with the high concentration of wells, seen in Fig. 3b, are

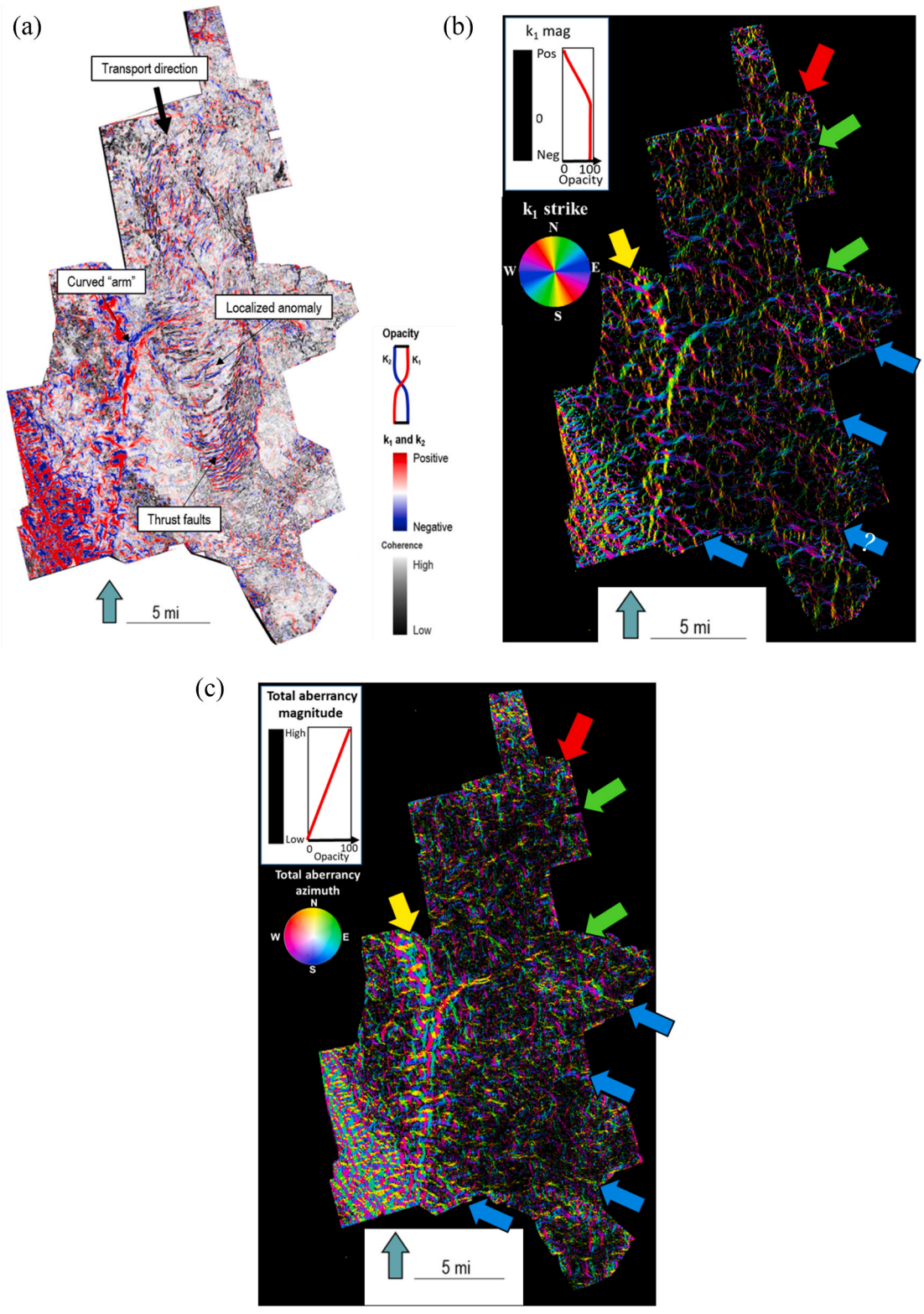

Fig. 8. (a) Co-rendered image of coherence with k_1 and k_2 anomaly along a mass transport deposit section in upper Leonardian (modified after Bhatnagar et al., 2019). On the base of San Andres, (b) k_1 strike modulated by k_1 magnitude, c) total aberrancy azimuth co-rendered with total aberrancy magnitude.

most likely the anticlinal closures, which are a result of strike-slip fault formation.

5.4. Production correlation

The deeper Early Paleozoic faults have a direct effect on the faults as well as natural fracturing in the shallower formations. Such faults and fractures create potential pathways of migration that impacts primary production as well as tertiary recovery methods. We analyzed the production of the available horizontal wells and the lineations observed on the aberrancy attribute extracted along the Woodford surface (Fig. 11). All of the available horizontal wells were drilled on the eastern margin

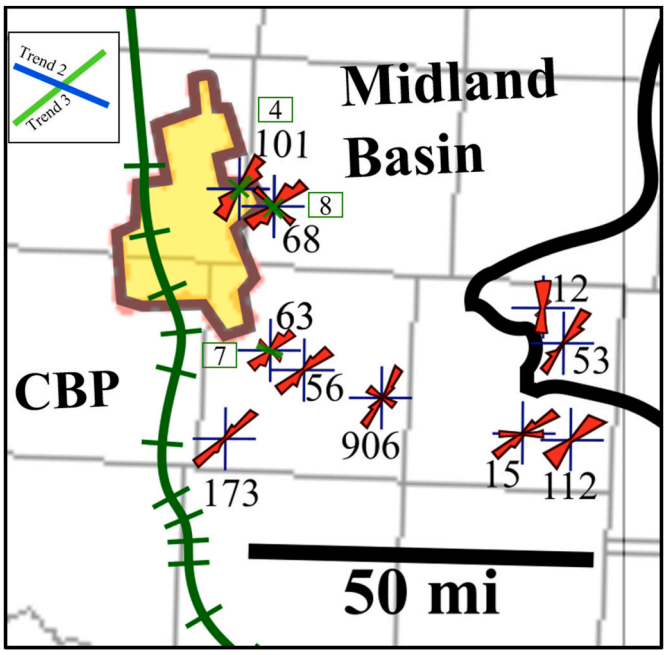

Fig. 9. Fracture orientation map near the study area in Midland Basin (modified from Forand et al., 2017). The map only shows the healed fractures. The red colored rose diagram, shows the orientation of different fracture sets. The green lines on top of the rose diagram shows the approximate direction of open fractures. The number next to the rose diagram shows the count of number healed fractures. The study area is indicated by a yellow polygon.

of the study area and landed in lower Permian (Wolfcamp and Spraberry) formations. The two criteria to evaluate these wells were the first one-year (12 months) hydrocarbon production (FYHP), which includes oil and gas, in terms of barrel of oil equivalent (BOE) and oil-water ratio (produced oil/produced water; OWR). The lateral length of horizontal wells range between 9000 ft and 11,000 ft. We have grouped different lateral wells into well groups (Well 1–6), based on their proximity. In order to normalize the FYHP and OWR, we took an average for each well group.

The first one-year production (FYHP) from the horizontal wells varies from the well to well. The best wells with the highest FYHP being the Well 3 and 4, but they have lower OWR values. Well 1, and 2 have the lower FYHP, but high OWR. The wells in south were completed less than a year ago so a true FYHP number is not available. We correlated FYHP and OWR with aberrancy. The wells drilled over areas of higher aberrancy have a lower OWR but a high FYHP.

The higher aberrancy magnitude corresponds to the areas of flexure, which can be potential fracture zones. A low OWR indicates that the amount of water is more than oil. In the case of higher FYHP and lower OWR, the oil volumes are more at the same time the volumes of the produced water are even more than other locations. We believe, the cause for such effect is the presence of higher permeability. In above-mentioned areas various fractures zones are present, such fractures continue to the shallower formation and connect to shallower producing formations. The water, as well as the hydrocarbon migrate via these factures.

6. Conclusions

In our study area, we have observed a complex strike-slip fault system, which includes fold and faults with dip-slip, oblique-slip, and purely strike-slip motion. Both, faults with significant and insignificant throws are present. Coherence illuminated the faults with enough throw, which shows a reflector break on the seismic amplitude section, e.g. trend 1 and trend 2. Coherence anomaly is absent for trend 3, which appears as a continuous reflector. Structural curvature and aberrancy illuminated all of the three trends. On the vertical seismic sections, all three trends have a shape of a monocline. We find, aberrancy, extremely useful, since it indicates the location of the point of inflection on these bends.

The structural elements observed in the CBP and Midland Basin, provides support of its developments as a right-lateral strike-slip system. The primary strike-slip fault is oriented in N 20°. The CPB axis is parallel to the fold axis of this strike-slip system. Trend 3 lineations represent R shear of the strike-slip system and align with ASZ, whereas R' shear

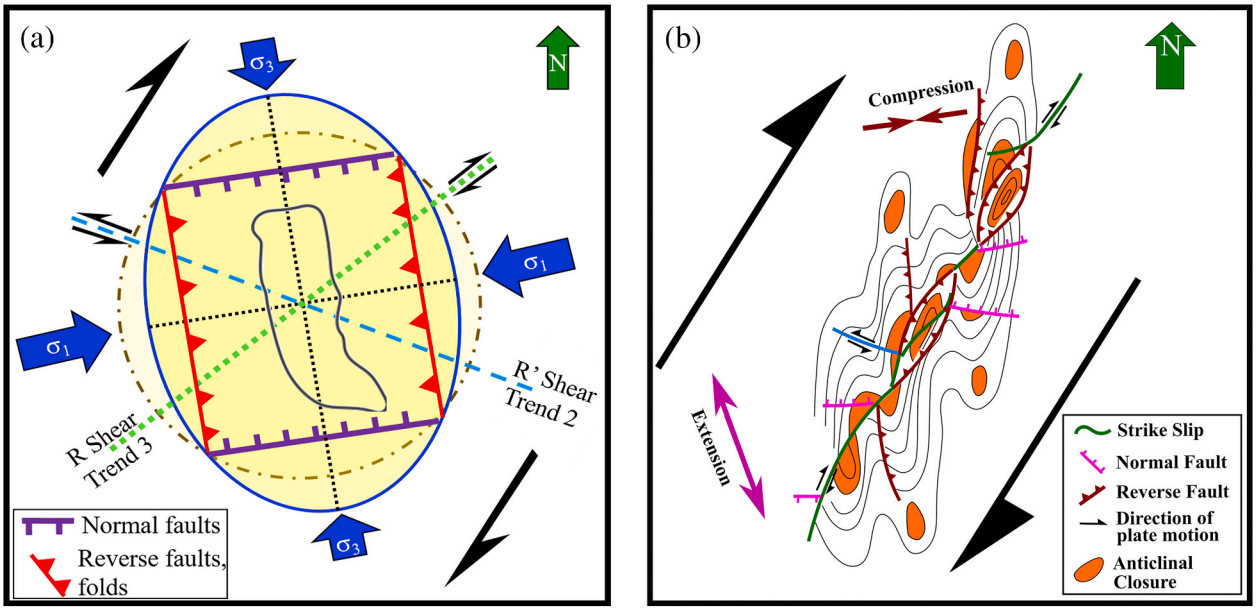

Fig. 10. (a) Right-lateral strike-slip fault system. Added the trend 2 (blue) and trend 3 (green), which matches the direction of R′ and R shear. In addition, in the middle, the Central Basin Platform out line is added to compare the orientation of CBP and the direction of principal stresses. (b) Intermediate stage of the evolution of right-lateral strike-slip fault system. The illustration includes different structural elements including strike-slip motion, normal fault, reverse fault, fold, anticlinal closures etc. (modified after Sylvester, 1988). Note, we have kept the orientation of the fault system, as per our interpretation of our results.

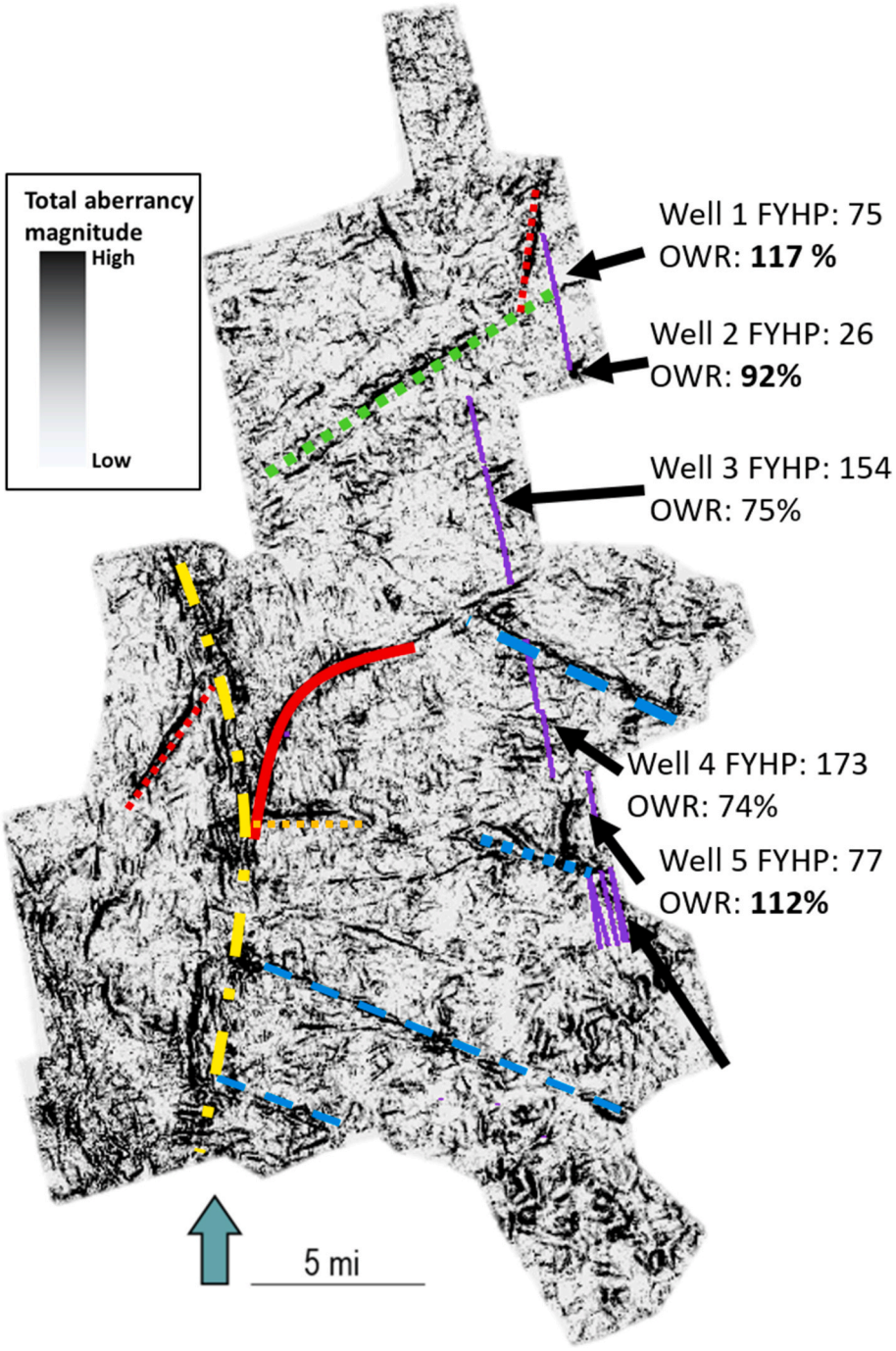

Fig. 11. Horizontal production wells on total aberrancy horizon slice along Woodford surface. The horizontal wells are displayed as solid purple lines. The FYHP stands for first year hydrocarbon production. FYHP number is represents kilo barrels of oil equivalent multiplied. For example, the well 1 has 75,000 barrels of oil equivalent production for the first year.

represents trend 2 lineations parallel to the NW trending surface lineaments. The structural evolution of both the ASZ and NW trending lineaments (trend 3) can be characterized by basement faults which have moved laterally. The formations above the basement were deformed in different stages, such characteristics can help to identify the timing of continued deformation and movement. The FMI logs-based study aids in confirming the structural elements seen with the seismic data. Most of the open fractures within the Midland Basin trend N 45° E. The high aberrancy values show the areas (of high flexure) where the rocks were under strain; these areas may be fracture zones. Theses fracture zones have higher permeability, and in such areas the drilled wells have lower OWR and FYHP. Drilling in the areas of high fractures would be economically profitable for a short term. Seismic attribute interpretation maps can be used to identification of areas of fracture zones and should be used in production well planning.

Credit author statement

Sumit Verma: Figure preparation, Writing - review & editing, Resources, Software, Validation, Data curation, Writing - original draft, Supervision, Methodology. **Matt Scipione:** Conceptualization, Methodology, Formal analysis, Writing - original draft.

Declaration of competing interest

The authors declare that they have no known competing financial interests or personal relationships that could have appeared to influence the work reported in this paper.

Acknowledgments

We would like to thank Fasken Oil and Ranch for the 3D seismic survey and well log donation to the UT Permian Basin. We thank Ron Bianco and Troy Tittlemire for their insightful advice. We used AASPI consortium's software to compute seismic attributes. We utilized Schlumberger's Petrel for interpretation, and Ikon Sciences' RokDoc for well log correlation.

Appendix A. Supplementary data

Supplementary data to this article can be found online at https://doi.org/10.1016/j.jngse.2020.103521.

References

Adams, D.C., Keller, R.G., 1996. Precambrian basement geology of the Permian Basin region of West Texas and eastern New Mexico: a geophysical perspective. AAPG (Am. Assoc. Pet. Geol.) Bull. 80, 410–431. https://doi.org/10.1306/64ED87FA-1724-11D7-8645000102C1865D.

Adams, D.C., Ouimette, M.A., Moreno, F., 1993. Middle-late Proterozoic extension in the Carlsbad region of southeastern New Mexico and west Texas. In: Love, D.W., Hawley, J.W., Kues, B.S., Austin, G.S., Lucas, S.G. (Eds.), New Mexico Geological Society 44th Annual Fall Field Conference Guidebook. New Mexico Geological Society, pp. 137–144.

Blumentritt, C.H., Sullivan, E.C., Marfurt, K.J., 2003. Channel detection using seismic attributes on the Central basin platform, West Texas. In: 73rd Annual International Meeting, SEG, Expanded Abstracts, pp. 466–469.

Ballard, J., 2014. Pre-Permian Structures of the Northern Central Basin Platform, Permian Basin, West Texas and Southeast New Mexico: ResearchGate. https://www.researchgate.net/publication/326017851_Pre-Permian_Structures_of_the_Northern_Central_Basin_Platform_Permian_Basin_West_Texas_and_Southeast_New_Mexico.

Bhatnagar, P., Verma, S., Bianco, R., 2019. Geomorphologic character of an Upper Leonardian mass transport deposit, Midland Basin: insights from 3D seismic data. Interpretation 7 (4), 1–14. https://doi.org/10.1190/INT-2019-0036.1.

Bhattacharya, S., Verma, S., 2019. Application of volumetric seismic attributes for complex fault network characterization on the north slope, Alaska. J. Nat. Gas Sci. Eng. 65, 56–67. https://doi.org/10.1016/j.jngse.2019.02.002.

Bhattacharya, S., Verma, S., 2020. Seismic attribute and petrophysics-assisted interpretation of the nanushuk and torok formations on the north slope, Alaska. Interpretation 8 (2). https://doi.org/10.1190/INT-2019-0112.1. SJ17-SJ34.

Bolden, G.P., 1984. Wrench faulting in selected areas of Permian Basin. AAPG (Am. Assoc. Pet. Geol.) Bull. 68 (1), 131–140. https://doi.org/10.1306/AD460981-16F7-11D7-8645000102C1865D.

Chopra, S., Marfurt, K.J., 2007. Seismic Attributes for Prospect Identification and Reservoir Characterization. Society of Exploration Geophysicists. Geophysical Developments No. #11.

EIA, 2018. Permian Basin Wolfcamp Shale Play, Geologic Review. https://www.eia.gov/maps/pdf/PermianBasin_Wolfcamp_EIAReport_Oct2018.pdf: browsed. (Accessed 2 October 2019).

Ewing, T.E., 2016. Texas through Time: Lone Star Geology, Landscapes, and Resources. The University of Texas at Austin, Bureau of Economic Geology Udden Series. No. 6.

Ewing, T.E., 2019. Tectonics of the West Texas (Permian) Basin—origins, structural geology, subsidence, and later modification. In: Ruppel, S.C. (Ed.), Anatomy of a Paleozoic Basin: the Permian Basin, USA: UT Austin, Bureau of Economic Geology Report of Investigations 285, pp. 63–96. AAPG Memoir 118.

Forand, D., Heesakkers, V., Schwartz, K., 2017. Constraints on Natural Fracture and In-Situ Stress Trends of Unconventional Reservoirs in the Permian Basin. Unconventional Resources Technology Conference, USA. https://doi.org/10.15530/URTEC-2017-2669208.

Gardiner, W.B., 1990. Fault fabric and structural sub-provinces of the Central basin Platform: a model for strike - slip movement. In: Flis, J.E., Price, R.C. (Eds.), Permian Basin Oil and Gas Fields: Innovative Ideas in Exploration and Development, vols. 90–87. West Texas Geological Society, pp. 15–27.

Hoak, T., Sundberg, K., Ortoleva, P., 1998. Overview of the Structural Geology and Tectonis of the Central Basin Platform, Delaware Basin, and Midland Basin. Science Applications International Corporation, West Texas and New Mexico.

Li, F., Qi, J., Lyu, B., Marfurt, K.J., 2017. Multispectral Coherence: Interpretation, 6 (1), T61–T69.

Mai, H.T., 2010. Seismic Attribute Analysis and its Application to Mapping Folds and Fractures. PhD Dissertation. The University of Oklahoma.

Marfurt, K.J., 2006. Robust estimates of 3D reflector dip and azimuth. Geophysics 71 (4), P29–P40.

Mosher, S., 1998. Tectonic evolution of the southern Laurentian Grenville orogenic belt. Geol. Soc. Am. Bull. 110 (11), 1357–1375. https://doi.org/10.1130/0016-7606(1998)110%3C1357:TEOTSL%3E2.3.CO;2.

Muehlberger, W.R., 1980. Texas lineament revisited. In: Dickerson, P.W., Hoffer, J.M., Callender, J.F. (Eds.), New Mexico Geological Society 31st Annual Fall Field Conference Guidebook. New Mexico Geological Society, pp. 113–121.

Marfurt, K.J., Alves, T., 2015. Pitfalls and limitations in seismic attribute interpretation of tectonic features: Interpretation, 3. https://doi.org/10.1190/INT-2014-0122.1. SB5-SB15.

Pollock, C., Seiler, C., Valcárcel, M., Macaulay, E., 2018. A Method of Fracture Prediction across Multiple Stratigraphic Horizons in the Midland Basin. Unconventional Resources Technology Conference, Texas, USA. https://doi.org/10.15530/URTEC-2018-2878217.

Pu, R., Li, K., Dong, M., Cao, Z., Xu, P., 2019. The 3D Seismic Characteristics and Significance of the Strike-Slip Faults in the Tazhong Area (Tarim Basin, China), Interpretation 7: T1-T19. https://doi.org/10.1190/INT-2016-0135.1.

Qi, X., Marfurt, K.J., 2018. Volumetric aberrancy to map subtle faults and flexures. Interpretation 6 (2), 1–64. https://doi.org/10.1190/INT-2017-0114.1.

Ruppel, S.C., 2019. Anatomy of a Paleozoic Basin: the Permian Basin. UT Austin, Bureau of Economic Geology, USA. AAPG Memoir 119.

Swan, M.M., 1976. The Stockton Pass Fault: an Element of the Texas Lineament. M. S. thesis. The University of Arizona.

Sylvester, A.G., 1988. Strike-slip faults. Geol. Soc. Am. Bull. 100, 1666–1703. https://doi.org/10.1130/0016-7606(1988)100<1666:SSF>2.3.CO;2.

Tai, P., Dorobek, S.L., 2000. Tectonic model for late paleozoic deformation of the Central Basin platform, Permian Basin region, and west Texas. In: DeMis, W.D., Nelis, M.K., Trentham, R.C. (Eds.), The Permian Basin: Proving Grounds for Tomorrow's Technologies. West Texas Geological Society Publication #109, pp. 157–176.

Verma, S., Del Moro, Y., Marfurt, K.J., 2013. Pitfalls in Prestack Inversion of Merged Seismic Surveys: Interpretation, vol. 1, pp. A1–A9. https://doi.org/10.1190/INT-2013-0024.1, 1.

Verma, S., Bhattacharya, S., Lujan, B., Agrawal, D., Mallick, S., 2018. Delineation of early Jurassic aged sand dunes and paleo-wind direction in southwestern Wyoming using seismic attributes, inversion, and petrophysical modeling. J. Nat. Gas Sci. Eng. 60, 1–10. https://doi.org/10.1016/j.jngse.2018.09.022.

Verma, S., Bhattacharya, S., 2019. Delineation of complex fault network North Slope, Alaska using seismic attributes. In: 89th Annual International Meeting, SEG, Expanded Abstracts, pp. 1893–1897. https://doi.org/10.1190/segam2019-3214607.1.

Yang, K.M., Dorobek, S.L., 1995. The Permian Basin of west Texas and New Mexico: tectonic history of a "composite'' foreland basin and its effect on stratigraphic development. In: Dorobek, S.L., Ross, G. (Eds.), Stratigraphic Evolution in Foreland Basins: SEPM Special Publication, 52. SEPM Special Publication, pp. 149–174.